C. R. Mecanique 341 (2013) 449–454

Contents lists available at SciVerse ScienceDirect

Comptes Rendus Mecanique

www.sciencedirect.com

10th International Meeting on Thermodiffusion

Formation of magnetoconvection by photoabsorptive methods in ferrofluid layers

Dmitry Zablotsky *, Ansis Mezulis, Elmars Blums

Institute of Physics, University of Latvia, Miera str. 32, Salaspils-1 LV-2169, Latvia

A R T I C L E I N F O

Article history:
Available online 27 February 2013

Keywords:
Forced Rayleigh scattering
Ferrofluids
Convection
Thermodiffusion

A B S T R A C T

A periodic concentration grating was induced in a layer of ferrofluid by photoabsorption and thermophoresis under the action of the applied uniform magnetic field. The application of the external field causes the appearance of an internal demagnetizing field within the layer and of magnetic forces due to the non-uniform distribution of concentration. The induced magnetic forces cause the appearance of parasitic microconvection within the layer. The experimental observations of the formation stage of the grating are interpreted to explain magnetoconvection, making use of numerical simulations.

1. Introduction

The investigation of the regimes of transport processes in different mediums, environments and ranges of parameters is of fundamental importance for their application in engineering and technology. Ferrofluids – stabilized colloidal dispersions of ferromagnetic nanoparticles in a liquid carrier – possess considerable magnetic properties and permit the magnetic mechanism of control over transport of heat and mass. One of the principle features is the formation of convective motion by magnetic forces – magnetoconvection. The perturbation of the ferrofluid magnetization by thermal non-uniformities or non-homogeneous distribution of the ferroparticle concentration leads to the emergence of thermomagnetic and magnetosolutal convection. On small length scales, the magnetic buoyancy mechanisms typically predominate over the conventional thermogravitational ones, even in constant fields.

The low diffusive mobility of the magnetic nanoparticles introduces important characteristics to the dynamics of the transport processes in strongly asymmetric magnetic dispersions. On the conventional length scales, the characteristic time of evolution of the stationary concentration profile is of the order of weeks and months. The thermal buoyancy mechanisms then dominate in the formation of convection on short timescales. However, the concentration dynamics determine exactly the long-term stability of the convective transport regime. In turn, on the submillimeter scale, the stationary concentration difference can be established in experimentally relevant time. The solutal mechanism of magnetic buoyancy is generally stronger than the thermal one and the development of magnetosolutal convection can be observed.

The formation of the desired shape of the concentration front is the major difficulty in the investigation of the magnetosolutal convection. Some of the first observations were concerned with the magnetoconvective destabilization of the diffusion front formed by bringing into contact magnetic fluids with different concentrations [1] or by magnetophoresis in strongly non-uniform magnetic fields [2]. The pronounced Soret effect and the considerable thermophoretic mobility, characteristic for the strongly asymmetric binary mixtures, permits the creation of the concentration fronts by thermal methods and the application of the temperature gradient. Both normal and anomalous thermodiffusion were observed in ferrocolloids with different methods of stabilization.

* Corresponding author.
E-mail address: Dmitrijs.Zablockis@gmail.com (D. Zablotsky).

1631-0721/$ – see front matter
http://dx.doi.org/10.1016/j.crme.2013.01.019

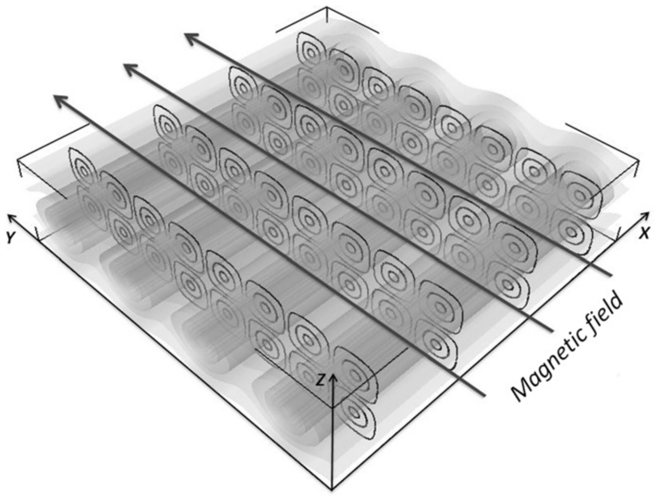

Fig. 1. Problem formulation: contours of the photoabsorptive grating and the shape of the magnetoconvective fluxes within the ferrofluid layer under parallel external field.

The photoabsorptive methods are most convenient for the formation of the concentration microstructures with the desired shape. The absorption of incident intensity by the ferroparticles allows transmitting the thermal energy to the whole volume of the ferrofluid layer within the penetration depth of the beam. The focusing of the optical radiation enables the creation of considerable thermal gradients and the corresponding concentration gradients, even at moderate beam intensities and temperature differences. Localized [3] or periodic microstructures [4–6] can be formed within the ferrofluid layer by different experimental arrangements.

The application of the external magnetic field to the photoabsorptive microstructures causes the ordering of the magnetic moments of the ferroparticles and the resulting non-homogeneity of the demagnetizing field. The interactions of the internal gradients of the concentration and magnetic field perturbations lead to the appearance of the magnetic force, which acts on the suspended phase. The resulting magnetophoretic motion can entrain the liquid carrier and cause the appearance of magnetic microconvection.

2. Formulation of the problem

When an optical grating with spatially periodic intensity of incident radiation is focused within a laterally unbounded ferrofluid layer, the corresponding photoinduced thermal modulation is created and the formation of the concentration non-homogeneities begins due to the thermophoretic effect (Fig. 1).

The influence of the photoabsorption within the volume of the layer can be modeled [7] by a periodic heat source $\propto \{1+\cos(\pi y)\}$ with the coefficient of proportionality $\frac{1}{2}\pi^2$ obtained from the normalization of the temperature field. The heat balance equation:

$$\Delta\delta T + \frac{1}{2}\pi^2\big\{1+\cos(\pi y)\big\} = 0 \tag{1}$$

determines the distribution of the temperature perturbation. The simple form of the boundary condition on the transversal sidewall of the layer corresponds to the Newton's law of cooling $\boldsymbol{n}\nabla\delta T + Bi\delta T = 0$, where the value of the Biot number $Bi = \frac{hL}{\lambda}$ has been taken equal to 1 for convenience. The approximate solution of the heat balance equation in a laterally unbounded layer can be obtained up to the leading lateral mode:

$$\delta T(y,z) = T_0(z) + T_1(z)\cos(\pi y) \tag{2}$$

with $T_0(z) = \frac{1}{4}\pi^2[\Delta^2 + 2\frac{\Delta}{Bi} - z^2]$ and $T_1(z) = \frac{1}{2}[1 - \frac{Bi\cosh(\pi z)}{\pi\sinh(\pi\Delta)+Bi\cosh(\pi\Delta)}]$.

The formation of the concentration non-homogeneities is driven by the three primary phoretic processes – the gradient diffusion, thermophoresis and magnetophoresis.

$$\boldsymbol{J}_c = -\nabla\delta c - s_T\nabla\delta T + \mathcal{M}_{\mathrm{ph}}\nabla\delta H \tag{3}$$

The magnetophoretic number $\mathcal{M}_{\mathrm{ph}} = \frac{\eta}{\rho_0 D}(1-c_0)\frac{m_g}{\eta f_v}\mu_0\chi_0 H_0\frac{\overline{\Delta H}}{\Delta c}$ governs the relative strength of the magnetophoresis and s_T – dimensionless Soret coefficient.

The evolution of the concentration microstructure is governed by the balance of the concentration fluxes:

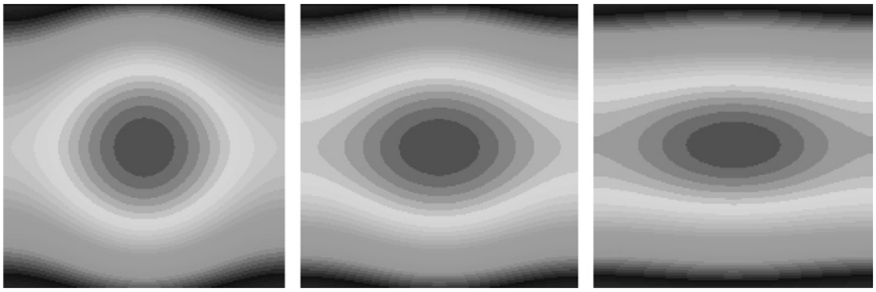

Fig. 2. Calculated profiles of the grating element: temperature distribution (left), concentration distributions at $Rs_{\mathrm{m}} = 0$ (middle) and $Rs_{\mathrm{m}} = 100$ (right).

$$\frac{\partial \delta c}{\partial t} = \Delta\{\delta c - \mathcal{M}_{\mathrm{ph}}\delta H + s_T\delta T\} - \boldsymbol{U}\nabla\delta c \tag{4}$$

$$-\nabla p + \Delta\boldsymbol{U} + \boldsymbol{f}_{\mathrm{m}} = 0 \tag{5}$$

with the volume density of the magnetic force $\boldsymbol{f}_{\mathrm{m}} = Rs_{\mathrm{m}}\delta c\nabla\delta H$. The control parameter is the magnetosolutal Rayleigh number $Rs_{\mathrm{m}} = \mu_0\chi_c\chi_0 H_0\frac{L^3}{\eta D}\overline{\Delta c}\frac{\overline{\Delta H}}{L}$.

The perturbation of the ferroparticle concentration creates the non-homogeneities of the internal demagnetizing field induced by the application of the external magnetic field. The perturbation of the magnetic scalar potential is determined from the magnetostatic Maxwell's equations:

$$\Delta\delta\psi = \tilde{\alpha}_c\boldsymbol{h}\nabla\delta c \tag{6}$$

as the magnetization of the ferrofluid is proportional to the concentration $\boldsymbol{\delta M} = \tilde{\alpha}_c\delta c\boldsymbol{h}$, with $\tilde{\alpha}_c = \chi_c\frac{\chi_0}{1+\chi_0}H_0\frac{\overline{\Delta c}}{\overline{\Delta H}}$ – dimensionless susceptibility.

The external scalar potential $\delta\varphi$ can be introduced, which describes the magnetic field in the free space outside the ferrofluid layer:

$$\Delta\delta\varphi = 0 \tag{7}$$

Assuming that the transversal boundary of the layer is impermeable to the flux of the ferroparticles and their deposition on the sidewall does not take place, the boundary condition on the slip-flux is obtained by $[\boldsymbol{n}\cdot\boldsymbol{J}_c = 0]_{\partial S}$. The non-slip boundary condition is imposed on the velocity field $[\boldsymbol{U} = 0]_{\partial S}$. The boundary condition for the scalar potentials follows from the requirement of the continuity of the magnetic field $[\frac{\partial}{\partial\boldsymbol{n}}\delta\psi = \tilde{\alpha}_c\delta c + \frac{\partial}{\partial\boldsymbol{n}}\delta\varphi]_{\partial S}$ and $[\delta\psi = \delta\varphi]_{\partial S}$. The set of equations can be solved by numerical methods, determining the distribution of the field perturbations within the element of the photoabsorptive grating (Fig. 2) and the time evolution of the microstructure.

3. Experiment

Since the diameter of the absorbing particles is 100...20 times less than the exciting wavelength, the optically induced grating setup is called forced Rayleigh scattering (FRS) (Fig. 3). We employ a continuous power Nd:YAG green light 532 nm laser as the incident source. This laser has maximal output power 1.5 W and allows low-frequency blocking through its electronic control unit that is used to measure the Soret coefficient.

The incident light has 1D sinusoidal spatial modulation with a period of ca. 100 μm, created by interference of two equal splitted beams. Due to the photoabsorption, a periodic temperature modulation appears within the sample that yields a periodic modulation of the nanoparticle volume concentration through the Soret effect. Thus, grating is induced by both temperature and particle volume fraction modulations, being examined by measuring the first-order diffracted intensity I_{d} of a low power He–Ne probe beam. As the values of the partial derivatives of the real part of refraction index $\partial n'/\partial c, \partial n'/\partial T$ in used ferrofluids are much larger than those of the imaginary part $\partial n''/\partial c, \partial n''/\partial T$, the diffracting grating is mainly an index one.

In accordance with linear optics, the diffracted amplitude E_{d} of an index grating is proportional to the sample thickness l and index modulation $\delta n'$:

$$E_{\mathrm{d}} = E_0\frac{2\pi l}{\lambda_{\mathrm{He-Ne}}}\delta n' \tag{8}$$

where $\delta n' = \frac{\partial n'}{\partial T}\delta T + \frac{\partial n'}{\partial c}\delta c$.

Quantitatively, the temperature and the concentration modulation are evaluated in some previous works with FRS [5,6]. For the present 1D sinusoidal case, it reads:

$$\delta T = \tau_{\mathrm{th}}WI_0; \qquad \delta c = -\tau_{\mathrm{th}}S_TWI_0 \tag{9}$$

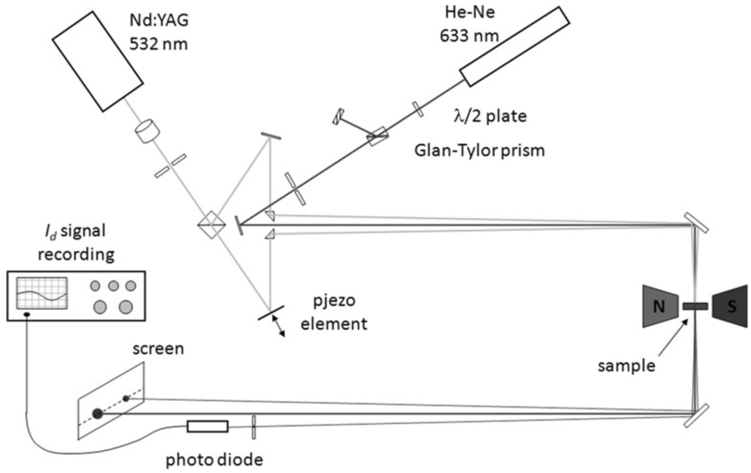

Fig. 3. Scheme of 1D forced Rayleigh scattering setup.

Table 1
Main dimensionless parameters for the series of experiments.

$\mathbf{B}_0 \parallel \nabla T$	0 mT	20 mT	30 mT	40 mT	60 mT	80 mT	120 mT
$\tilde{\alpha}_c$	–	1	1	1	1	1	1
$\mathcal{M}_{ph}$	–	0.01	0.02	0.03	0.05	0.08	0.12
s_T	–	1.01	1.02	1.03	1.05	1.08	1.13
Rs_m	–	5	11	16	30	43	62
$\frac{\Delta c[H]}{\Delta c[0]}$	1.0	0.99	0.98	0.97	0.95	0.92	0.89

where the photoabsorptive efficiency $W = \frac{1-e^{-a_p l}}{l\rho c_p}$, a_p being the absorption coefficient of the sample, and I_0 is the incident light intensity ($\approx 10^4$ W/m^2). The characteristic thermal relaxation time is defined as $\tau_{th} = \frac{\rho c_p}{\lambda q^2}$, with q the spatial wavenumber.

Neglecting here any incoherent noise, $E_d/E_0 = \sqrt{I_d/I_0}$, and the diffracted intensity can be expressed as:

$$\sqrt{\frac{I_d}{I_0}} = \frac{2\pi l}{\lambda_{He-Ne}} \tau_{th} W I_0 \left(\frac{\partial n'}{\partial T} - \frac{\partial n'}{\partial c} S_T \right) \tag{10}$$

With the examined ferrofluid samples $\sqrt{I_d/I_0} \approx 0.02 \ldots 0.05$, which is enough with the probe He–Ne beam of $I_0 = 10 \ldots$ 20 mW to see the first-order diffracted spot with the human eye, which makes easier adjusting the optical detection setup.

4. Analysis

The values of the dimensionless parameters calculated for the intensities of the magnetic field employed in the series of experiments are summarized in Table 1.

Fig. 4 shows the time dependence of the square root of the measured diffracted intensity in a series of experiments with different field strengths. The value of this quantity is proportional to the magnitude of first lateral mode of the induced concentration perturbation. The value $\sqrt{I_d}$ is compared to the L^2-norm:

$$J(t) = \sqrt{\int_{-\Delta}^{\Delta} \left\{ \int_{-1}^{1} \delta c(y, z, t) \cos(\pi y)\, dy \right\}^2 dz} \tag{11}$$

which is obtained from the calculations.

The time evolution of $J(t)$ (Fig. 4) is obtained from the simulations of the formation stage of the concentration grating for the parameters in Table 1. Much information can be gained from the comparison between experimental and calculated data. For convenience, all series have been normalized by the corresponding zero-field saturation values.

The notable evidence of the influence of microconvective transport is the somewhat relaxational character of the measured diffracted signal after the initially attained maximum. In fact, despite rather small values of the magnetic solutal Rayleigh numbers, such behavior cannot be explained by any phoretic process and is a clear sign of microconvection. Comparing the calculated and measured time dependencies of the appropriate quantities, it is possible to conclude that the

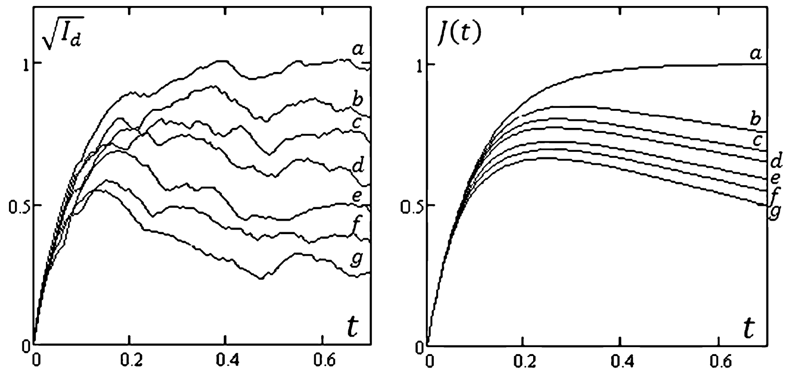

Fig. 4. Formation of the concentration grating, establishing of the stationary state in the lateral applied field: experimental measurements of the diffracted intensity (left) and numerical calculations (right) at (a) zero field (b) 20 mT, (c) 30 mT, (d) 40 mT, (e) 60 mT, (f) 80 mT, (g) 120 mT.

correspondence is not perfect, but is still acceptable, taking into account the absence of the approximation parameters. Certainly, the qualitative comparison is possible at the least.

One of the main factors for the quantitative discrepancy between the calculations and the experimental measurements seems to be the polydispersity of the studied sample. The magnetic core size distribution can be obtained by the method of magnetic granulometry. In fact the magnetic diameters were approximately in the range between 5 and 10 nm. This leads to two notable conclusions. First of all, larger magnetic nanoparticles have greater magnetophoretic mobility. Secondly, the relative contribution of the certain size fraction to the diffracted intensity is proportional to the sixth power of its diameter $\sim d^6$. Then the visibility of the larger particles is far greater than that of the smaller ones.

Considering the dynamics of the evolution of the grating, it seems that the presence of microconvection significantly slows down the formation of the stationary state, especially at lower values of the magnetic solutal Rayleigh numbers as compared with the phoretic process alone. At higher fields, the evolution of the measured diffracted signal reaches the stationary state rather quickly, somewhat faster than predicted by the theory. It can then be concluded that in this case the effective value of the Rayleigh number is greater than the one predicted taking into account the presence of some contributing factor. Additional calculations show that the observed rapid establishing of the stationary regime takes place at $Rs_{\mathrm{m}} \sim 250$. Such discrepancy can be explained by the deformation of the assumed symmetric configuration of the perturbations with respect to the midplane of the layer, since the dependence of the solutal Rayleigh number on the characteristic length is very strong. For the purpose of gaining understanding of the dynamics of the measured diffracted signal during the formation stage of the concentration grating, it is appropriate to consider the microscopic evolution of the photoabsorptive convective–diffusive microstructures. In the large aspect ratio structures, the formation of the concentration profile begins at the boundary, regardless of the sign of the Soret coefficient. Initially, the interaction of the concentration boundary layer with the gradient of the corresponding demagnetizing field creates two sets of convective rolls near the opposite sidewalls of the ferrofluid layer (Fig. 5). The concentration front, which is advanced by the interaction of the thermophoretic and magnetophoretic fluxes, then, drives these rolls to the center of the layer, all the while the microconvection acting to homogenize the concentration perturbation that creates it and slows down the evolution of the concentration profile.

If the symmetry of the field perturbations across the midplane of the layer is broken, then the asymmetric contributions cannot be neglected anymore. Qualitatively this means that one of the pairs of the convective rolls will begin to suppress the other pair with the increase of the control parameter, leading to the increase of the effective Rayleigh number for the dominating set of rolls. In fact, the measurements of the intensity of the beam exiting the ferrofluid layer show considerable decrease as compared with the entering beam, which can well lead to the asymmetry of the field perturbations. Unfortunately, the present model cannot account for the asymmetric terms, but their presence does not seem to change the qualitative picture of the process.

5. Conclusions

The measurements of the diffracted intensity from the formation stage of the photoabsorptive concentration grating in parallel magnetic field show notable discrepancies with the predictions of the phoretic model accounting for the gradient diffusion, thermophoresis and magnetophoresis as the only contributing effects. The observed peculiarities can be interpreted in terms of magnetoconvective transport emerging due to the interactions of the perturbation of the concentration field with the corresponding gradients of the demagnetizing field induced by the application of the external magnetic field. The numerical simulations with account for the formation of the magnetosolutal microconvection within the photoabsorptive grating allow us to explain the qualitative behavior of the measured diffracted intensity during the creation of the grating.

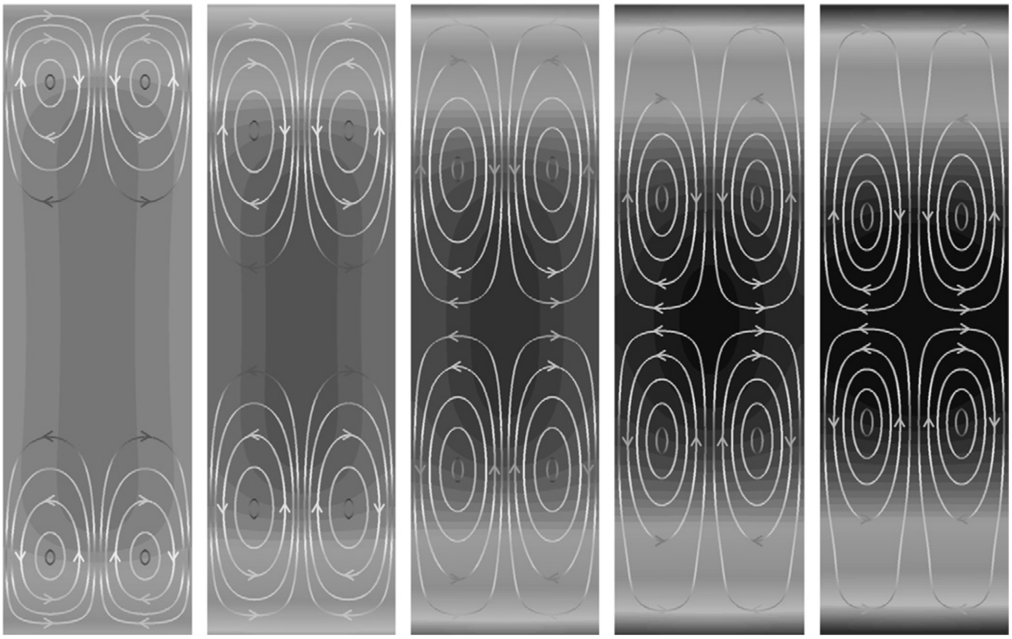

Fig. 5. Formation of the concentration grating, establishing of the stationary state in the lateral applied field of 120 mT. The calculated contours of the concentration field and convective streamlines at times $t = 0.2, 0.4, 0.6, 0.8, 1.0$.

Acknowledgements

The work has been supported by the European Social Fund within the project “Support for Doctoral Studies at University of Latvia” and the European Regional Development Fund, project 2011/0001/2DP/2.1.1.1.0/10/APIA/VIAA/007.

References

[1] M.M. Maiorov, A.O. Tsebers, Magnetic microconvection on the diffusion front of the ferroparticles, Magnetohydrodynamics 19 (1983).
[2] A.Yu. Chukhrov, Convective stability of dilute colloid in the presence of magnetic diffusion in an inhomogeneous field, Magnetohydrodynamics 22 (1986).
[3] W. Luo, T. Du, J. Huang, Novel convective instabilities in a magnetic fluid, Phys. Rev. Lett. 82 (1999).
[4] J.C. Bacri, A. Cebers, A. Bourdon, G. Demouchy, B.M. Heegaard, R. Perzynski, Forced Rayleigh experiment in a magnetic fluid, Phys. Rev. Lett. 74 (1995).
[5] J. Lenglet, A. Bourdon, J.-C. Bacri, G. Demouchy, Thermodiffusion in magnetic colloids evidenced and studied by forced Rayleigh scattering experiments, J. Phys. Rev. E 65 (2002) 031408.
[6] G. Demouchy, A. Mezulis, A. Bee, D. Talbot, J.-C. Bacri, A. Bourdon, Diffusion and thermodiffusion studies in ferrofluids with a new two-dimensional forced Rayleigh scattering technique, J. Phys. D. Appl. Phys. 37 (2004) 1417–1428.
[7] D. Zablotsky, E. Blums, Relaxation mechanisms of photoinduced periodic microstructures in ferrofluid layers, Phys. Rev. E 84 (2011).